Vietnam Journal of Science and Technology ***58*** *(6) (2020) 747-759*

doi:10.15625/2525-2518/58/6/15259

SIMULATION OF DIRECT CONTACT MEMBRANE DISTILLATION REGENERATION OF LIQUID DESICCANT SOLUTIONS USED IN AIR-CONDITIONING

Duong Cong Hung[1,*], Tran Thi Thu Lan[2]

[1]*Le Quy Don Technical University, 236 Hoang Quoc Viet, Bac Tu Liem, Ha Noi, Viet Nam*

[2]*Institute of Environmental Technology, Vietnam Academy of Science and Technology, 18 Hoang Quoc Viet, Cau Giay, Ha Noi, Viet Nam*

[*]Email: *hungduongcong@gmail.com*

Received: 8 July 2020; Accepted for publication: 15 October 2020

Abstract. Membrane distillation (MD) has great potential for the treatment of hyper saline waters, including liquid desiccant solutions used in air-conditioning systems. Previous experimental investigations have demonstrated the technical feasibility of MD for regeneration of liquid desiccant solutions. In this study, a direct contact membrane distillation (DCMD) process of the LiCl liquid desiccant solution was simulated using MATLAB software. The simulation was first validated with the data obtained from experimental tests. Then, it was used to elucidate the feed and distillate temperatures, LiCl concentration, and water flux profiles along the membrane leaf inside the DCMD membrane module. Finally, with the help of the simulation, the effects of membrane properties and process operating conditions on the DCMD process performance were systematically examined. The results obtained from this simulation enrich the knowledge and hence facilitate the realization of MD for the liquid desiccant solution regeneration application.

*Keywords***:** membrane distillation; liquid desiccant air conditioner; regeneration of liquid desiccant solutions; process simulation.

Classification numbers: 3.7.1, 3.8.1.

1. INTRODUCTION

Membrane distillation (MD) has emerged as promising technology platform for strategic desalination applications, including the regeneration of liquid desiccant solutions used in air-conditioning systems [1, 2]. The MD process combines thermal distillation with membrane separation; therefore, it has advantages of both thermal distillation and membrane processes. In MD, a hydrophobic microporous membrane is used to separate a hot saline solution from a cold distillate (i.e. fresh water): liquid water cannot permeate through the membrane pores, but water vapor can, resulting in a complete rejection of non-volatile dissolved salts in the saline solution. This means that the MD process can produce super-pure distillate from any sources of saline waters if the membrane pores are not wet [3, 4]. The transfer of water vapor through the MD

membrane pores is driven by a vapor pressure gradient generated by a temperature difference between the two sides of the membrane. Thus, provided that the saline solution is heated while the distillate is cooled, water can transfer from the saline solution to the distillate in vapor form inside the membrane pores. The saline solution can be concentrated, and pure distillate can be obtained at the same time. Low-grade heat sources such as waste heat from industrial processes or solar thermal can be used to heat the saline solution in the MD process to reduce its energy costs. As a result, a great number of solar-driven or waste heat-driven MD desalination processes have been trialed and reported in the literature for various water treatment applications such as seawater desalination [5 - 8], waste brine concentration [9, 10], and particularly regeneration of liquid desiccant solutions for air-conditioning [11].

Regeneration of liquid desiccant solutions has a vital role in sustaining the efficiency of liquid desiccant air-conditioning (LDAC) systems, and the MD process has been experimentally demonstrated for this strategic application [12-17]. The LDAC process consists of two cycles: air dehumidification and liquid desiccant solution regeneration [2, 18]. In the air dehumidify cation cycle, the concentrated liquid desiccant solution absorbs moisture from the air to dehumidify and cool the air. The moisture absorption, however, dilutes and heats up the liquid desiccant solution, reducing its dehumidification capacity. Thus, in the regeneration cycle, the diluted liquid desiccant solution is reconcentrated and cooled to restore its dehumidification capacity. Liquid desiccant solutions can be regenerated using several methods, amongst which MD has been considered the most ideal process given its compatibility with the hyper salinity of liquid desiccant solutions [2]. Experimental investigations have proven the feasibility of MD regeneration of liquid desiccant solutions – the MD process at the feed temperature of 65 °C could regenerate the liquid desiccant LiCl solution up to 29 wt.% (i.e. the saturation concentration of LiCl solution at 25 °C is about 42 wt.%) without any issues of membrane wetting, and simultaneously obtain high quality distillate for beneficial reuse [15, 17]. It is necessary to note that liquid desiccant LiCl solutions near saturation exhibit elevated dehumidification capacity, but are more prone to salt crystallization that might lead to blocking of liquid channels inside the air dehumidifier and regenerator. Various MD configurations have been deployed in these experimental investigations, most notably including direct contact membrane distillation (DCMD). This is because DCMD is the simplest and most widely used configuration reported in the literature [4, 19].

Experimental studies are vital for the feasibility demonstration of the MD process for regeneration of liquid desiccant solutions. They pave the way for further studies to facilitate the realization of MD for this strategic application. Experimental works can be conducted to optimize the MD process of liquid desiccant solutions; however, they require considerable costs and time to achieve workable results. In this context, simulation using computer software can be a feasible approach. Indeed, there have been a great number of simulation studies on the MD process for seawater desalination as summarized in a review article [20]. It is noteworthy that there has not been any reported work regarding the simulation and optimization of the MD process for regeneration of liquid desiccant solutions used for air-conditioning systems.

This study aimed to simulate the DCMD regeneration of a liquid desiccant solution used in air-conditioners. The selected liquid desiccant solution was LiCl solution given its most popular use for liquid desiccant air conditioners. The simulation was built using MATLAB and validated with experimental testing. The simulation was then used to examine the effects of membrane properties and process operating conditions on the performance of the DCMD process.

2. THEORIES AND SIMULATION APPROACHES

2.1. Theories

During the DCMD process of the LiCl solution, water and heat are simultaneously transferred through the membrane from the feed to the distillate. Water flux (J) through the membrane is calculated as below [4, 21]:

$$J = C_m \left(P_{f.m} - P_{d.m} \right) \tag{1}$$

where C_m is the membrane mass transfer coefficient, $P_{f.m}$ and $P_{d.m}$ are the water vapor pressure at the feed and distillate membrane surface, respectively. C_m depends on membrane properties and water vapor temperature inside the membrane pores as expressed below [4, 22]:

$$C_m = \left[\frac{3}{2} \frac{\tau\delta}{\varepsilon r} \left(\frac{\pi RT}{8M} \right)^{1/2} + \frac{\tau\delta}{\varepsilon} \frac{P_a}{PD} \frac{RT}{M} \right]^{-1} \tag{2}$$

where τ, δ, ε, and r are respectively the membrane pore tortuosity, membrane thickness, membrane porosity, and pore radius; P and P_a are the total pressure and the air partial pressure inside the membrane pore; R is the gas constant; D is the water diffusion coefficient; M is the molecular weight of water; and T is the mean water vapor temperature inside the membrane pores. Water vapor pressure of the feed and distillate at the membrane surfaces (e.g. $P_{f.m}$ and $P_{d.m}$) can be calculated as [4]:

$$P_{d.m} = \exp\left(23.1964 - \frac{3816.44}{T_{d.m} - 46.13} \right) \tag{3}$$

$$P_{f.m} = x_{water} a_{water} \exp\left(23.1964 - \frac{3816.44}{T_{f.m} - 46.13} \right) \tag{4}$$

where $T_{f.m}$ and $T_{d.m}$ are respectively the water temperature at the feed and distillate membrane surfaces, x_{water} and a_{water} are water molar fraction and water activity of the LiCl solution. Water molar fraction and water activity of the LiCl solution are functions of the LiCl concentration (S) as below [23]:

$$x_{water} = 1 - \frac{18S}{18S + 42.4(100 - S)} \tag{5}$$

$$a_{water} = 1 - 0.9139 \times 10^{-2} S - 3.5169 \times 10^{-4} S^2 \tag{6}$$

where S is in percentage (%).

During the DCMD process, heat transfer occurs in three regions: from the hot feed to the membrane, across the membrane, and from the membrane to the cold distillate. Details about the heat transfer mechanism and the governing equations to calculate the heat transfer in these three regions can be found elsewhere [4, 20]. Based on the heat conservation rule, the water temperature at the feed and distillate membrane surfaces (e.g. $T_{f.m}$ and $T_{d.m}$) can be calculated using the following equations:

$$T_{f.m} = \frac{T_{f.b}h_f + h_m\left(T_{d.b} + T_{f.b}\dfrac{h_f}{h_d}\right) - J\Delta H_v}{h_f\left(1+\dfrac{h_m}{h_d}\right)+h_m} \tag{7}$$

$$T_{d.m} = \frac{T_{d.b}h_d + h_m\left(T_{f.b} + T_{d.b}\dfrac{h_d}{h_f}\right) + J\Delta H_v}{h_d\left(1+\dfrac{h_m}{h_f}\right)+h_m} \tag{8}$$

where h_f, h_d, h_m are the heat transfer coefficient of the feed, distillate, and the membrane, respectively; $T_{f.b}$ and $T_{d.b}$ are the water temperature in the bulk feed and distillate; J is the water flux; and ΔH_v is the latent heat of water evaporation. The heat transfer coefficients are functions of thermodynamic properties of feed and distillate streams and the membrane properties. The calculations the heat transfer coefficients and bulk feed and distillate temperatures (e.g. $T_{f.b}$ and $T_{d.b}$) are provided in [8].

As demonstrated in the Eq. (1), $T_{f.m}$ and $T_{d.m}$ are required for the calculation of water flux (J); however, in the Eq. (7) & (8) J is involved in the calculation of $T_{f.m}$ and $T_{d.m}$. In this situation, iteration must be deployed for the calculation of J, $T_{f.m}$, and $T_{d.m}$. This means that $T_{f.m}$ and $T_{d.m}$ are first assigned with the value of $T_{f.b}$ and $T_{d.b}$, respectively, for the calculation of J; and then the calculated J is used for the calculation of new $T_{f.m}$ and $T_{d.m}$. The iteration is repeated until the differences between new $T_{f.m}$ and $T_{d.m}$ and those previously set values approach to zero. Details about the iteration process can be found in the study by Duong *et al*. [8].

2.2. Simulation approaches

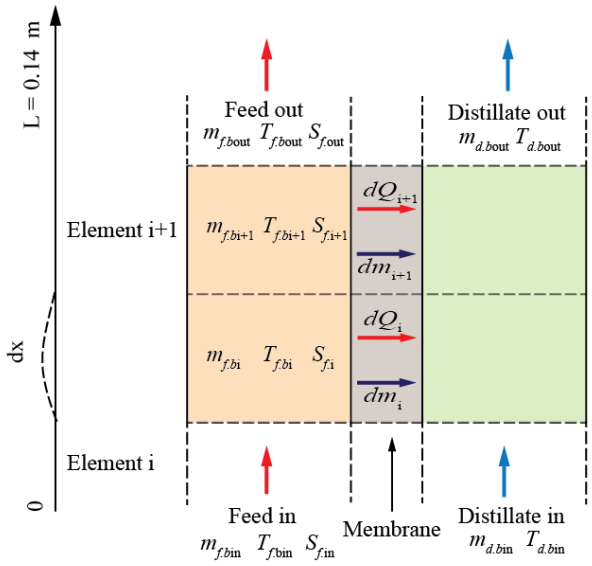

Figure 1. Schematic diagram of the two incremental membrane elements (e.g. *i* and *i+1*) along the membrane leaf inside the DCMD membrane module. The process is under co-current flow mode.

The DCMD process of the LiCl solution feed is simulated using 1D model with the support of MATLAB software. Water temperatures of the feed and distillate in the bulk and at the membrane surfaces, LiCl solution concentration, and water flux along the membrane channel from the inlet to the outlet can be profiled. To enable the simulation, the membrane leaf is divided into small membrane elements, and the heat and mass transfer (e.g. *dQ* and *dm*) through each membrane element are calculated using Eq. (1-8) (Fig. 1). The mass flow rate (*m*), bulk fluid temperature (*T*), and bulk LiCl concentration (*S*) are calculated based on the mass and heat conservation.

Inputs to the simulation include membrane properties (e.g. membrane thickness, membrane porosity, and membrane pore size), membrane module specifications (e.g. feed and distillate channel length, width, and height), and process operating conditions (e.g. feed and distillate inlet temperature, feed and distillate cross-flow velocity, and LiCl concentration). Otherwise stated, the default values of these inputs are set for each simulation run and provided in Table 1.

Experimental DCMD tests with the 20 % LiCl solution with the operating conditions, membrane properties, and membrane module specifications stated in Table 1 were conducted to validate the simulation. During the tests, distillate was returned to the feed tank to maintain the constant concentration of the LiCl solution. The feed tank was covered and sealed on the top to prevent the moisture exchange between the LiCl solution and the surrounding environment. Electrical conductivity of the obtained distillate was measured using a conductivity meter (Hatch, USA) to ensure that no membrane pore wetting had occurred during the validation. Water flux of the DCMD process for each test was measured using a plastic graduated cylinder at stable conditions for at least 1 hour. Temperatures of the feed and distillate were regulated using a heating element and a chiller, respectively.

Table 1. The default membrane properties, membrane module specifications, and process operating conditions used in the simulation of the DCMD process of the LiCl solution.

Process simulation inputs	**Default value**
Membrane properties:	
Membrane thickness (μm)	60
Membrane porosity (%)	80
Membrane pore diameter (μm)	0.2
Membrane module specifications:	
Membrane length (m)	0.14
Membrane width (m)	9.5
The channel height (m)	2×10^{-3}
Process operating conditions:	
Feed inlet temperature (°C)	70
Distillate inlet temperature (°C)	20
Feed and distillate inlet cross-flow velocity ($m.s^{-1}$)	0.03
LiCl concentration (%)	20

3. RESULTS AND DISCUSSIONS

3.1. Validation of the DCMD process simulation

Water flux is one the most important process performance parameters of the DCMD process of the LiCl liquid desiccant solution; therefore, it is used as an indicator to validate the simulation program. Even though feed and distillate outlet temperatures can also be relied on for the simulation validation, they are excluded in this study. As shown in Fig. 2, the simulated process water flux using the computer program well agreed with the experimentally measured flux during the DCMD regeneration of the 20 % LiCl liquid desiccant solution. The deviations between the simulated and the experimentally measured process water flux were less than 5 %, indicating the high accuracy of the simulation program. Moreover, both simulation and experimental results confirm the exponential relationship between the process water flux and the feed operating temperature: elevating the feed inlet temperature led to an exponential increase in the DCMD process water flux. This relationship has been well-established in the MD literature regarding both seawater desalination and liquid desiccant solution regeneration applications [17, 24].

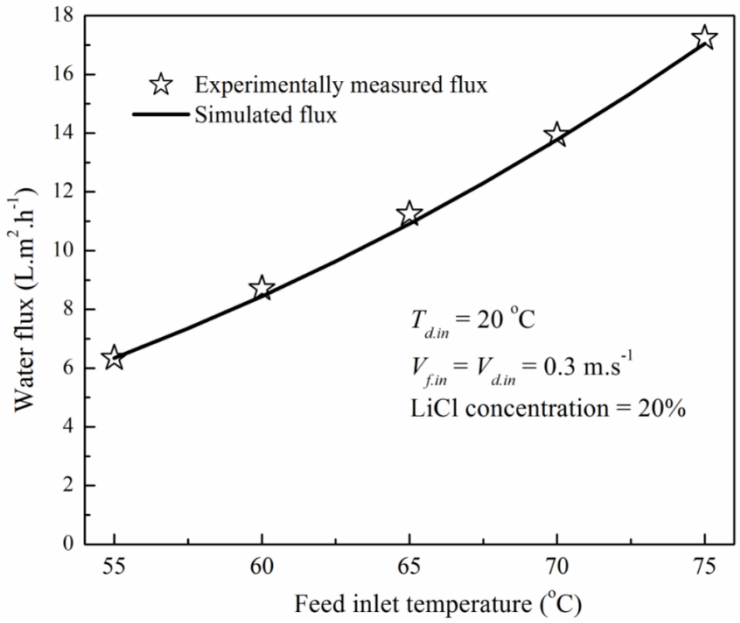

Figure 2. Experimentally measured and simulated water flux of the DCMD process with the 20 % LiCl liquid desiccant solution at various feed inlet temperature. Other operating conditions: Other operating conditions: distillate inlet temperature $T_{d.in}$ = 20 °C, feed and distillate inlet cross flow velocity $V_{f.in}$ = $V_{d.in}$ = 0.03 m.s^{-1}.

3.2. Water temperature, solution concentration, and water flux profiles inside the DCMD membrane module

In experimental studies, water flux of the DCMD process along the membrane channel inside the membrane module cannot be depicted, otherwise the average process water flux is obtained by measuring the weight of the distillate produced in a time interval. In this study, the simulation program involves the heat and mass transfer through every elements of the membrane leaf inside the membrane module; thus, it allows for the detailed description of water

temperatures, water flux, and LiCl concentration along the membrane leaf inside the membrane module.

Along the membrane leaf inside the membrane module, the temperature of the LiCl solution feed gradually decreases while the distillate temperature steadily increases from the inlet to the outlet of the DCMD membrane module (Fig. 3). This is due to the heat transfer from the feed to the distillate along the membrane leaf. During the DCMD process, the heat is transferred across the membrane from the hot feed to the cold distillate via conduction through the membrane matrix and the latent heat associated with the water vapor flux. For most DCMD processes, the heat transferred through the membrane is comparable to the sensible heat of the feed and distillate, resulting in noticeable decline in feed solution temperature and rise in distillate temperature.

The heat transfer from the feed to the distillate also results in the formation of thermal boundary layers adjacent to the membrane surfaces on the feed and distillate side of the membrane. These thermal boundary layers cause the LiCl solution temperature at the membrane surface ($T_{f.m}$) lower than in the bulk feed ($T_{f.b}$), while the distillate temperature at the membrane surface ($T_{d.m}$) is higher than in the bulk distillate ($T_{d.b}$). This is defined as temperature polarization in the DCMD process. Largely, temperature polarization renders the water temperature difference between the feed and distillate membrane surfaces (ΔT_m) smaller than that between the bulk feed and distillate (ΔT_b), thus negatively affecting the process water flux. The simulation results shown in Fig. 3 reveal a considerable temperature polarization effect during the DCMD process of the 20 % LiCl solution. When operating under feed and distillate inlet temperature of 70 °C and 20 °C, respectively, ΔT_m is about 10 °C lower than ΔT_b (Fig. 3). It is noteworthy that the temperature polarization effect is an intrinsic issue of DCMD because this process is non-isothermal, and the heat transfer is always associated with the flux of water vapor through the membrane.

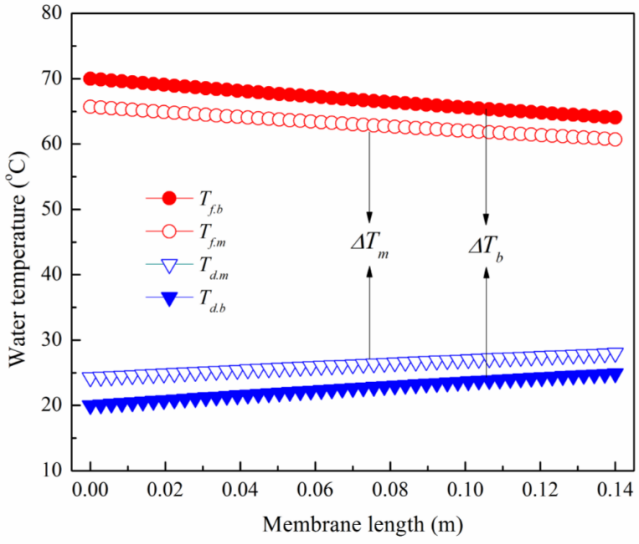

Figure 3. Simulated temperature profiles of the feed and distillate streams along the membrane leaf inside the membrane module during the DCMD process of the 20 % LiCl solution. Operating conditions: feed inlet temperature $T_{f.in}$ = 70 °C, distillate inlet temperature $T_{d.in}$ = 20 °C, feed and distillate inlet cross-flow velocity $V_{f.in} = V_{d.in}$ = 0.03 m.s^{-1}.

Consistent with the feed and distillate temperature profiles, water flux decreases along the membrane leaf inside the membrane module from the inlet to the outlet when the feed and distillate flow co-currently. As demonstrated in Fig. 4, water flux declines by approximately 30 % from 16.5 $L.m^{-2}.h^{-1}$ at the inlet to 11.5 $L.m^{-2}.h^{-1}$ at the outlet of the module, whereas the temperature difference between the LiCl feed and distillate at the membrane surface (ΔT_m) decreases by 21 % from 41.4 °C to 32.7 °C (Fig. 3). The non-linear declining rates between water flux and ΔT_m along the membrane leaf are attributed to the exponential relation between water vapor pressure and water temperature as demonstrated in the Eq. (3 and 4). In the DCMD process, the water vapor pressure difference between the feed and distillate membrane surfaces is the actual driving force for the transfer of water vapor through the membrane. In the case of a constant ΔT_m, the DCMD process operated at higher temperature achieves a higher water flux than that operated at lower temperature.

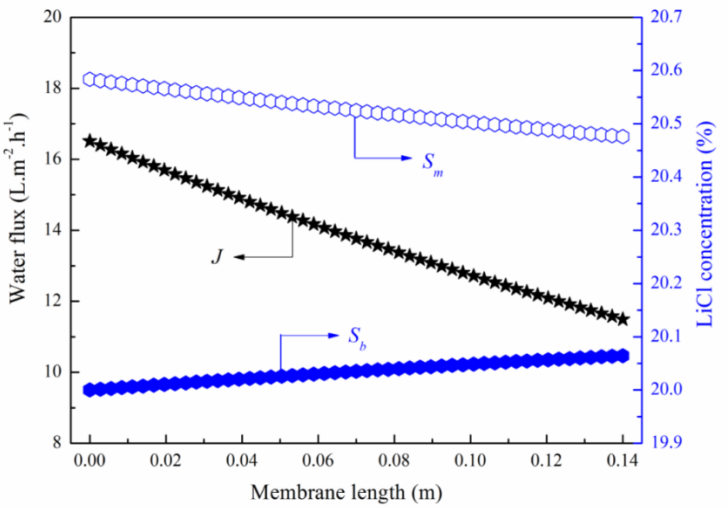

Figure 4. Simulated water flux (J) and LiCl concentration at the membrane surface (S_m) and in the bulk solution (S_b) along the membrane leaf inside the membrane module during the DCMD process of the 20 % LiCl solution. Operating conditions: feed inlet temperature $T_{f.in}$ = 70 °C, distillate inlet temperature $T_{d.in}$ = 20 °C, feed and distillate inlet cross-flow velocity $V_{f.in} = V_{d.in}$ = 0.03 $m.s^{-1}$.

Due to the transfer of water through the membrane, the LiCl concentration in the bulk feed (S_b) increases along the membrane length from the inlet to the outlet of the membrane module (Fig. 4). After travelling through the feed channel of the DCMD module, the LiCl concentration slightly increases from 20 % to 20.05 %. This slight increase in the LiCl concentration is expected as a short membrane leaf of 0.14 m is used for this DCMD simulation. For practical DCMD processes, the membrane leaf can be as long as 1.5 m, then the increase in the LiCl concentration after undergoing the DCMD regeneration process can be higher.

The simulation results also reveal a discernible magnitude of concentration polarization during the DCMD regeneration of the 20 % LiCl solution. The LiCl concentration at the feed membrane surface (S_m) is much higher than that in the bulk feed (S_b) (Fig. 4). As dissolved LiCl salt in the feed solution reduces its water vapor pressure, the concentration polarization effect together with temperature polarization negatively affects the water flux of the DCMD process of the LiCl solution feed. The detailed contribution of concentration and temperature polarization effects on the DCMD process water flux during the regeneration of the 20 % LiCl solution has been elucidated in a recent study by Duong *et al*. [23].

3.3. Effects of membrane properties and process operating conditions on water flux during the DCMD regeneration of the LiCl solution

One notable advantage of the DCMD process simulation compared with experimental studies is the ability to examine the effects of membrane properties and process operating conditions on the process performance. In this section, the impacts of membrane properties and process operating conditions on the process water flux during the DCMD regeneration of LiCl solution will be clarified. The process water flux is the average of all local water flux calculated along the membrane leaf inside the membrane module as reported in the section 3.2.

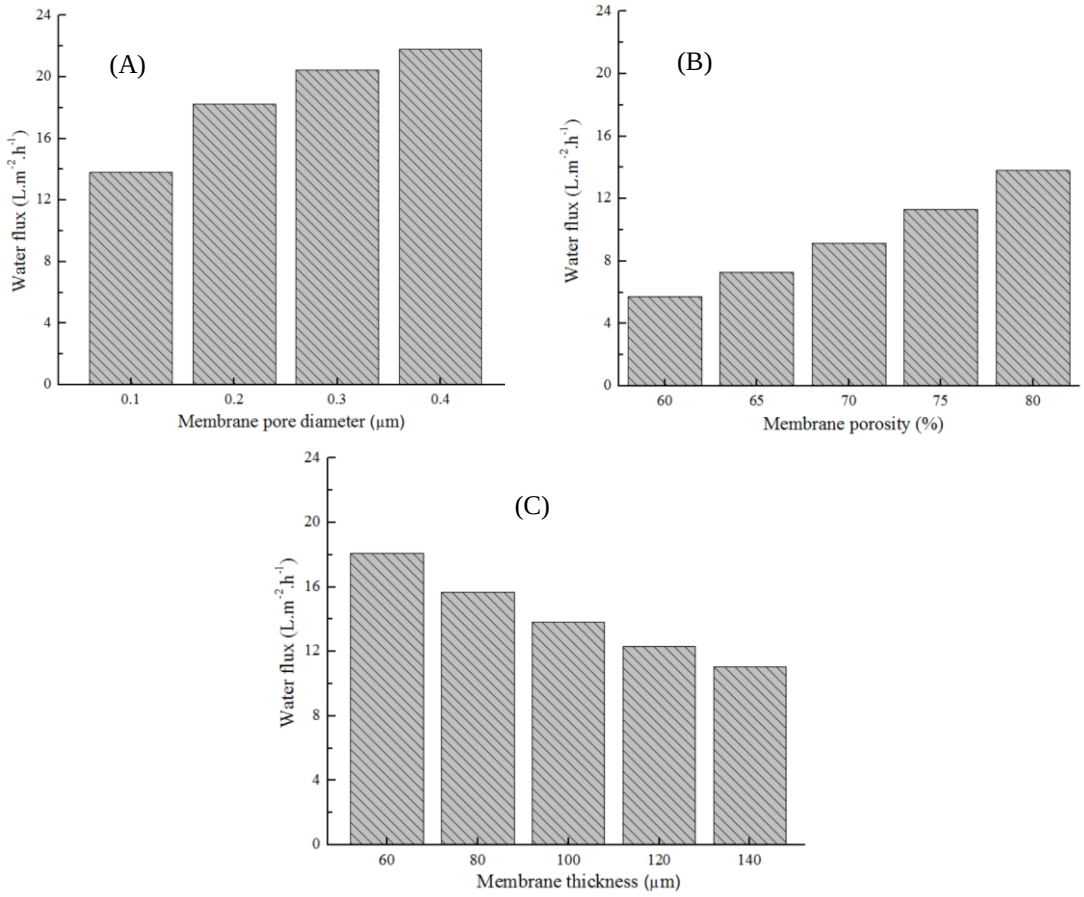

Figure 5. Effects of (A) membrane pore size, (B) membrane porosity, and (C) membrane thickness on water flux of the DCMD process with the 20 % LiCl solution feed. Operating conditions: feed inlet temperature $T_{f.in}$ = 70 °C, distillate inlet temperature $T_{d.in}$ = 20 °C, feed and distillate inlet cross flow velocity $V_{f.in}$ = $V_{d.in}$ = 0.03 m.s^{-1}.

The simulated water flux of the DCMD process with the 20 % LiCl solution feed using the membrane with different pore size, porosity, and thickness is demonstrated in Fig. 5. The DCMD process using membrane with larger pores achieves higher water flux (Fig. 5A). Similarly, the process with a more porous membrane favors the increased water flux (Fig. 5B). This is because the membrane with larger pore size and porosity offers larger areas for water evaporation and vapor condensation respectively at the feed and distillate membrane surfaces, thus improving the process water flux. It is, however, noteworthy that membranes with larger

pore sizes are more prone to membrane pore wetting than those with smaller pores, while increased membrane porosity compromises the mechanical strength of the membrane. As a result, most MD processes reported in the literature use membranes with pore sizes in the range of 0.1 - 0.4 μm and porosity from 60 % to 80 % [4].

Opposite to membrane pore size and porosity, increasing membrane thickness leads to a reduction in the simulated DCMD process water flux (Fig. 5C). Thicker membrane means a longer distance for water vapor to travel through the membrane from the LiCl feed to the distillate. As a result, water flux of all MD processes reported in the literature is inversely proportional to the membrane thickness. Therefore, regarding water flux, thin membranes are desired for the MD process. Nevertheless, thin membranes are associated with more conductive heat transfer from the feed to the distillate, resulting in reduced thermal efficiency of the DCMD process. As a result, the optimal membrane thickness for the DCMD process has been reported to be about 60 μm [4].

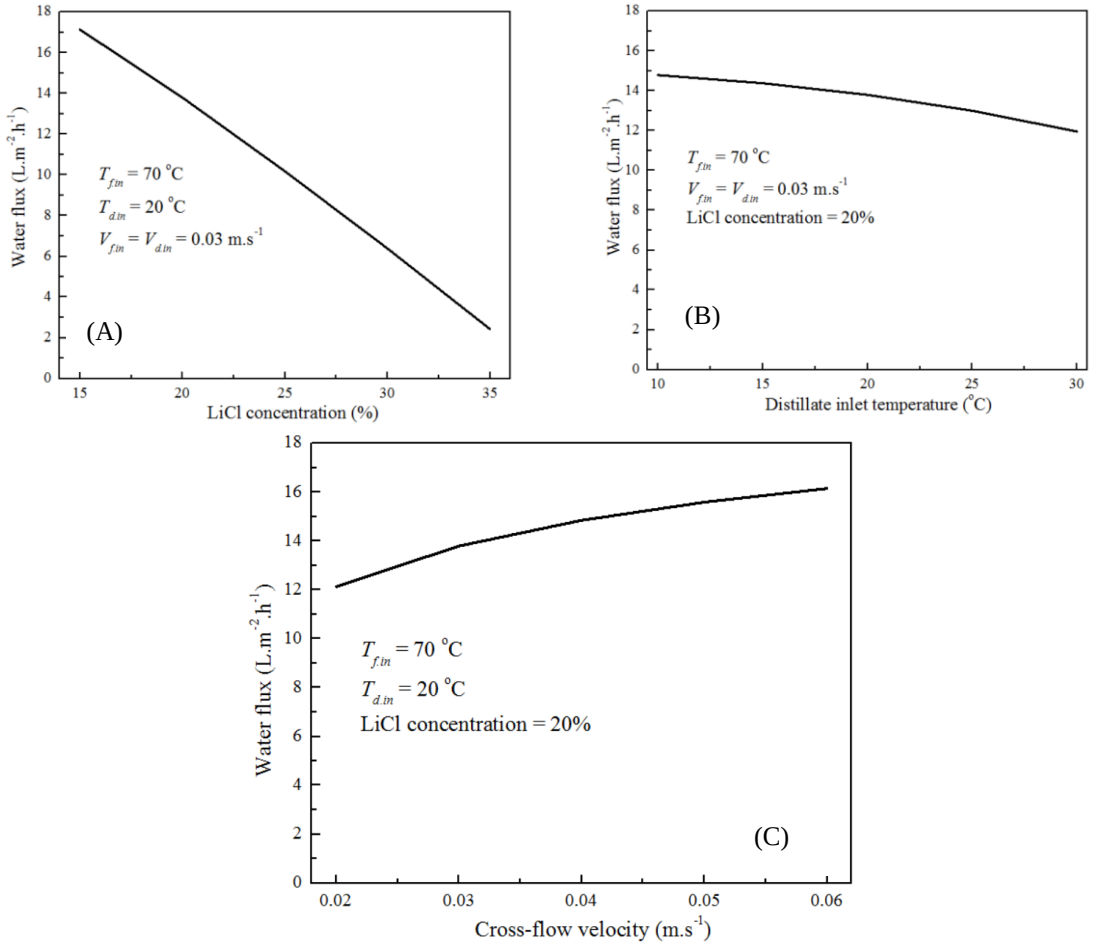

Figure 6. Effects of (A) LiCl concentration, (B) distillate inlet temperature, and (C) feed and distillate inlet cross-flow velocities on water flux during the DCMD process of LiCl solution feed.

Water flux of the DCMD process with the LiCl solution feed is also affected profoundly by the process operating conditions. Amongst the three variable operating conditions (e.g. LiCl

concentration, distillate temperature, and feed and distillate cross-flow velocity), LiCl concentration exerts the most profound impact on the DCMD process water flux (Fig. 6A). Elevating the LiCl concentration from 15 % to 35 % results in a marked decline in the process water flux, dropping from 17 $L.m^{-2}.h^{-1}$ to 2 $L.m^{-2}.h^{-1}$. Increasing the distillate temperature also leads to a reduction in the process water flux, but at a much lower extent compared with the effect of the LiCl concentration (Fig. 6B). On the other hand, increasing feed and distillate cross-flow velocity enhances the DCMD process water flux (Fig. 6C). This is because increasing cross-flow velocity promotes the hydraulic turbulence adjacent to the membrane surfaces, enhances the heat and mass transfer in the boundary layers, and mitigates the negative effects of temperature and concentration polarization, thus elevating the DCMD process water flux [25]. Nevertheless, the effect of increasing feed and distillate cross-flow velocity on the process water flux is not comparable to that of the temperature and concentration of the LiCl solution feed. Also, excessively increasing feed and distillate cross-flow velocity might lead to membrane pore wetting, which is a serious technical challenge to the DCMD regeneration of LiCl solution. Increasing feed and distillate cross-flow velocity also entails higher electric energy consumption of water circulating pumps [26].

4. CONCLUSIONS

In this study, the simulation of a DCMD process with the LiCl liquid desiccant solution feed was simulated using codes built in MATLAB. The simulation exhibited high accuracy as its simulated water flux well matched with the data obtained in the experimental tests. Given the accuracy of the simulation, detailed water temperatures, LiCl concentration, and water flux profiles along the membrane leaf inside the DCMD membrane module could be depicted. Along the short membrane leaf of 0.14 m long, feed and distillate temperatures greatly varied, leading to a significant decline in water flux by 30 %, dropping from 16.5 $L.m^{-2}.h^{-1}$ at the inlet to 11.5 $L.m^{-2}.h^{-1}$ at the outlet of the module. The simulation also allowed for evaluating the effects of membrane properties and process operating conditions on the water flux of the DCMD regeneration of the LiCl liquid desiccant solution.

Acknowledgements. This research is funded by Le Quy Don Technical University under project number 19.1.003.

REFERENCES

1. Duong H. C., Ansari A. J., Hailemariam R. H., Woo Y. C., Pham T. M., Ngo L. T., Dao D. T., and Nghiem L. D. - Membrane Distillation for Strategic Water Treatment Applications: Opportunities, Challenges, and Current Status, Current Pollution Reports **6** (2020) 173-187.
2. Duong H. C., Ansari A. J., Nghiem L. D., Cao H. T., Vu T. D., and Nguyen T. P. - Membrane Processes for the Regeneration of Liquid Desiccant Solution for Air Conditioning, Current Pollution Reports **5** (2019) 308-318.
3. Rezaei M., Warsinger D. M., Lienhard V. J. H., Duke M. C., Matsuura T., and Samhaber W. M. - Wetting phenomena in membrane distillation: Mechanisms, reversal, and prevention, Water Research **139** (2018) 329-352.
4. Alkhudhiri A., Darwish N., and Hilal N. - Membrane distillation: A comprehensive review, Desalination **287** (2012) 2-18.

5. Li G. and Lu L. - Modeling and performance analysis of a fully solar-powered stand-alone sweeping gas membrane distillation desalination system for island and coastal households, Energy Conversion and Management **205** (2020) 112375.
6. Li Q., Beier L. J., Tan J., Brown C., Lian B., Zhong W., Wang Y., Ji C., Dai P., Li T., Le Clech P., Tyagi H., Liu X., Leslie G., and Taylor R.A. - An integrated, solar-driven membrane distillation system for water purification and energy generation, Applied Energy **237** (2019) 534-548.
7. Andrés-Mañas J. A., Ruiz-Aguirre A., Acién F. G., and Zaragoza G. - Assessment of a pilot system for seawater desalination based on vacuum multi-effect membrane distillation with enhanced heat recovery, Desalination **443** (2018) 110-121.
8. Duong H. C., Xia L., Ma Z., Cooper P., Ela W., and Nghiem L. D. - Assessing the performance of solar thermal driven membrane distillation for seawater desalination by computer simulation, Journal of Membrane Science **542** (2017) 133-142.
9. Dow N., Gray S., Li J.D., Zhang J., Ostarcevic E., Liubinas A., Atherton P., Roeszler G., Gibbs A., and Duke M. - Pilot trial of membrane distillation driven by low grade waste heat: Membrane fouling and energy assessment, Desalination **391** (2016) 30-42.
10. Duong H. C., Chivas A.R., Nelemans B., Duke M., Gray S., Cath T. Y., and Nghiem L. D. - Treatment of RO brine from CSG produced water by spiral-wound air gap membrane distillation - A pilot study, Desalination **366** (2015) 121-129.
11. Choo F. H., KumJa M., Zhao K., Chakraborty A., Dass E. T. M., Prabu M., Li B., and Dubey S. - Experimental Study on the Performance of Membrane based Multi- effect Dehumidifier Regenerator Powered by Solar Energy, Energy Procedia **48** (2014) 535-542.
12. Zhou J., Wang F., Noor N., and Zhang X. - An experimental study on liquid regeneration process of a liquid desiccant air conditioning system (LDACs) based on vacuum membrane distillation, Energy **194** (2020) 116891.
13. Gurubalan A., Maiya M.P., and Tiwari S. - Experiments on a novel membrane-based liquid desiccant dehumidifier for hybrid air conditioner, International Journal of Refrigeration **108** (2019) 271-282.
14. Lefers R., Bettahalli N. M. S., Fedoroff N., Nunes S.P., and Leiknes T. - Vacuum membrane distillation of liquid desiccants utilizing hollow fiber membranes, Separation and Purification Technology **199** (2018) 57-63.
15. Duong H. C., Álvarez I. R. C., Nguyen T. V., and Nghiem L. D. - Membrane distillation to regenerate different liquid desiccant solutions for air conditioning, Desalination **443** (2018) 137-142.
16. Chen Q., Kum Ja M., Li Y., and Chua K. J. - Thermodynamic optimization of a vacuum multi-effect membrane distillation system for liquid desiccant regeneration, Applied Energy **230** (2018) 960-973.
17. Duong H. C., Hai F. I., Al-Jubainawi A., Ma Z., He T., and Nghiem L. D. - Liquid desiccant lithium chloride regeneration by membrane distillation for air conditioning, Separation and Purification Technology **177** (2017) 121-128.
18. Gurubalan A., Maiya M. P., and Geoghegan P. J. - A comprehensive review of liquid desiccant air conditioning system, Applied Energy **254** (2019) 113673.
19. Drioli E., Ali A., and Macedonio F. - Membrane distillation: Recent developments and perspectives, Desalination **356** (2015) 56-84.

20. Hitsov I., Maere T., De Sitter K., Dotremont C., and Nopens I. - Modelling approaches in membrane distillation: A critical review, Separation and Purification Technology **142** (2015) 48-64.
21. Duong H. C., Cooper P., Nelemans B., Cath T. Y., and Nghiem L. D. - Optimising thermal efficiency of direct contact membrane distillation by brine recycling for small-scale seawater desalination, Desalination **374** (2015) 1-9.
22. Duong H. C., Phan N. D., Nguyen T. V., Pham T. M., and Nguyen N. C. - Membrane distillation for seawater desalination applications in Vietnam: potential and challenges, Vietnam Journal of Science and Technology **55** (2017) 659-682.
23. Duong H. C., Ansari A. J., Cao H. T., Nguyen N. C., Do K. U., and Nghiem L. D. - Membrane distillation regeneration of liquid desiccant solution for air-conditioning: Insights into polarisation effects and mass transfer, Environmental Technology & Innovation **19** (2020) 100941.
24. Duong H. C., Duke M., Gray S., Cooper P., and Nghiem L. D. - Membrane scaling and prevention techniques during seawater desalination by air gap membrane distillation, Desalination **397** (2016) 92-100.
25. Srisurichan S., Jiraratananon R., and Fane A. G., Mass transfer mechanisms and transport resistances in direct contact membrane distillation process, Journal of Membrane Science **277** (2006) 186-194.
26. Duong H. C., Cooper P., Nelemans B., Cath T. Y., and Nghiem L. D. - Evaluating energy consumption of air gap membrane distillation for seawater desalination at pilot scale level, Separation and Purification Technology **166** (2016) 55-62.